Geomechanics and Engineering, *Vol. 10, No. 1 (2016) 77-94*
DOI: http://dx.doi.org/10.12989/gae.2016.10.1.077

An experimental investigation on dynamic properties of various grouted sands

Darn-Horng Hsiao [1], Vu To-Anh Phan [*2] and Chi-Chang Huang [1]

[1] Department of Civil Engineering, National Kaohsiung University of Applied Sciences, No. 415 Chien Kung Road, Kaohsiung 80778, Taiwan R.O.C.
[2] Faculty of Civil Engineering, Ton Duc Thang Univeristy, No. 19 Nguyen Huu Tho, Ho Chi Minh City, Vietnam

(*Received December 09, 2014, Revised July 10, 2015, Accepted November 03, 2015*)

Abstract. Cyclic triaxial and resonant column tests were conducted to understand the beneficial effects of various grouted sands on liquefaction resistance and dynamic properties. The test procedures were performed on a variety of grouted sands, such as silicate-grouted sand, silicate-cement grouted sand and cement-grouted sand. For each type of grout, sand specimen was mixed with a 3.5% and 5% grout by volume. The specimens were tested at a curing age of 3, 7, 28 and 91 days, and the results of the cyclic stress ratio, the maximum shear modulus and the damping ratio were obtained during the testing program. The influence of important parameters, including the type of grout, grout content, shear strain, confining pressure, and curing age, were investigated. Results indicated that sodium silicate grout does not improve the liquefaction resistance and shear modulus; however, silicate-cement and cement grout remarkably increased the liquefaction resistance and shear modulus. Shear modulus decreased and damping ratio increased with an increase in the amplitude of shear strain. The effect of confining pressure on clean sand and sodium silicate grouted sand was found to be insignificant. Furthermore, a nonlinear regression analysis was used to prove the agreement of the shear modulus-shear strain relation presented by the hyperbolic law for different grouted sands, and the coefficients of determination, R^2, were nearly greater than 0.984.

Keywords: silicate-grouted sand; cement-grouted; silicate-cement grouted sand; dynamic properties

1. Introduction

Over the past few decades, soil liquefaction has been one of the most interesting and complex phenomenon occurring during the seismic loading of earthquakes. Soil liquefaction can cause severe damage to various types of buried soil-structures. Based on the knowledge obtained from recent research and case studies around the world on the causes and effects of liquefaction, scholars have drawn conclusions regarding the types of soils that are most susceptible to failure and the liquefaction procedure. Generally, the phenomenon frequently related to cohesionless soils is the one that increases the pore water pressure and reduces the effective confining pressure. The result is a sudden reduction in the shear modulus of the soil, which, in turn, results in increased soil deformation and a loss in bearing strength. In the case of full liquefaction, when an increase in the pore water pressure reduces the effective stress to zero, the soil experiences a full loss of

*Corresponding author, Ph.D., E-mail: phantoanhvu@tdt.edu.vn; phantoanhvu@yahoo.com

http://www.techno-press.org/?journal=gae&subpage=5 ISSN: 2005-307X (Print), 2092-6219 (Online)

strength and undergoes large viscous deformations (Sladen *et al*. 1985).

To mitigate the liquefaction risk, the use of remedial measures is most likely the only available option for several existing structures that have been constructed in liquefiable soil areas. Practically, chemical grouting can be used to mitigate the liquefaction (Maher *et al*. 1994a) and may be one of the most effective methods. Generally, the physical and engineering properties of poor soil conditions, such as the strength, hydraulic conductivity, volume stability, stiffness, and undrained shear strength, which are related to the liquefaction potential, can be significantly improved using the chemical grouting technique. Furthermore, the widespread use of the grouting method demands a profound understanding of the characteristics and behavior of grouted materials, including the dynamic properties.

Thus far, certain chemical grouts have been popularly used, such as cement-, micro-fine cement-, sodium silicate-, colloidal silica-, and mineral-grout. For cement grout, although fewer dynamic tests have been performed, compared with static tests of cemented soil properties, literature reviews indicated that ordinary Portland cement was used to significantly improve the liquefaction resistance and the stiffness of the soil (Acar and El-Tahir 1986, Chen and Lin 2003, Dupas and Pecker 1979, Haeri *et al*. 2005, Saxena *et al*. 1988b, Tsai and Ni 2012).

Micro-fine cement grout first appeared in Japan approximately 30 years ago and has become commonly available. The advantage of this material is that it not only has better flow properties and bleed characteristics compared to that of ordinary Portland cement grout but it also easily permeates medium-to-coarse sands (Mollamahmutoglu and Yilmaz 2011, Mollamahmutoglu *et al*. 2007). (Maher *et al*. 1994a) described that the micro-fine cement caused the sand to not experience any initial liquefaction or a 5% cyclic mobility over the stress ratio and the cyclic numbers test ranges. (Delfosse-Ribay *et al*. 2004) revealed that micro-fine grouting improves the stiffness by a factor of 4. (Pantazopoulos and Atmatzidis 2012) concluded that micro-fine cement grouted sands obtained a higher shear modulus, initial Young's modulus and damping ratio values compared with those of sands grouted with ordinary cements by 25%-40%.

Certain results indicated that the use of colloidal silica grouted sand substantially improved the liquefaction potential and cyclic undrained behavior of loose sand (Gallagher and Mitchell 2002). Similarly, (Liao *et al*. 2004) used colloidal silica as grouting material to improve the liquefaction resistance of in-situ sandy soil. The test results indicated that the liquefaction resistance of grouted sand increased up to 4- to 7-fold compared with that of ungrouted sand. A higher stress ratio and a greater number of loading cycles were needed to initial in grouted sand specimens. In particular, sand stabilized with colloidal silica grout significantly increased its unconfined compression strength using long-term curing (Persoff *et al*. 1999, Yonekura and Miwa 1993).

Sodium silicate grout has been developed into a variety of different systems and is widely used as a chemical grout. In practice, sodium silicate grout systems usually consist of sodium silicate and a hardener, which can be used to effectively obtain the strong bonding properties in a two-compound system (Kazemian *et al*. 2012). However, the study of the dynamic properties of sodium silicate is still limited and not fully understood (Chang and Woods 1987, Delfosse-Ribay *et al*. 2004, Gonzalez and Vipulanandan 2007, Hsiao *et al*. 2014, Tsai and Ni 2012, Vipulanandan and Ata 2000). Delfosse-Ribay *et al*. (2004) conducted a few tests on sodium silicate grout composed of sodium silicate and an organic hardener and revealed that when sand was grouted with sodium silicate grout, the average improvement was 3 times larger compared with that obtained using clean sand. Additionally, the shear modulus of the grouted sand is higher than that of sand. (Tsai and Ni 2012) presented the results of an experiment comparing the sodium silicate-cement stabilized soil with cement stabilized soil and slag cement stabilized soil. The results indicated that the maximum shear modulus of the cement stabilized soil increases with increasing confining pressure, the minimum damping ratio decreases with increasing confining pressure, and the sodium silicate-cement stabilized soil was able to sustain a larger shear strain before incurring stiffness degradation compared with the other types of additives.

In Taiwan, sodium silicate grout is typically used to improve soft soil conditions. Using this material has several advantages, such as its reliability, proven performance, safety and ease of use, environmental acceptability, and low cost. Additionally, the use of sodium silicate grout significantly increases the permeability during the grout pumping process. Thus far, it has been observed that there are no reports on the use of only sodium silicate, and limited results exist for the dynamic properties of silicate-cement grouted sand. The objective of this study is to present the experimental results of the cyclic triaxial and resonant column tests for sand grouted with various grouts, such as sodium silicate, cement, and sodium silicate combined with cement. A series of cyclic triaxial and resonant column tests were conducted to determine the liquefaction resistance, maximum shear modulus, shear modulus, normalized shear modulus and damping ratio. The effects of grouting treatment content, type of grout, various combination grout content, shear strain, confining pressure and curing time on liquefaction resistance, shear modulus and damping ratio were evaluated in this study. The work also included one case study that was part of the broader research; this study was performed on the conformity of locally available soils for construction in Kaohsiung, Pingtung County, Taiwan. The experimental data would be used as the quantitative basis for further design recommendations in the area.

2. Materials

2.1 Sand

The natural soil used in this experimental investigation was obtained from the Li-Gang river shore in Kaohsiung, Pingtung County, Taiwan. Based on ASTM D422-2007, a quantity of natural soil was carefully sieved to obtain the grain size distribution curve, as indicated in Fig. 1. A specific gravity test was conducted in accordance with ASTM D854-2010 to determine a Gs value of 2.7. The basic physical properties of the sand used in the laboratory are summarized in Table 1. Based on the Unified Soil Classification System ASTM D2487-2000, this soil can be classified as well-graded sand (SW).

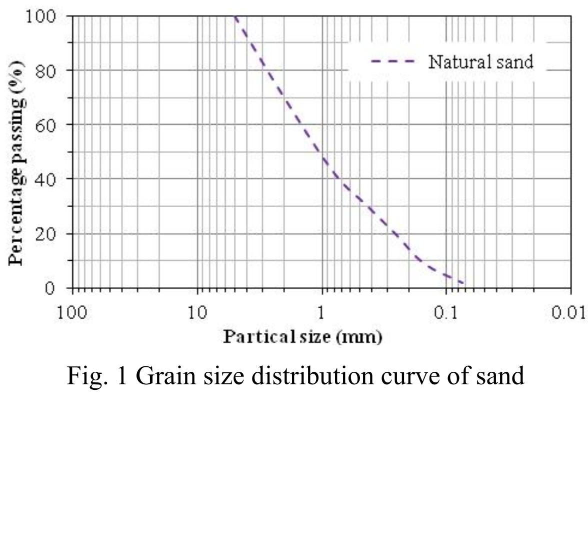

Fig. 1 Grain size distribution curve of sand

Table 1 Basic-physical properties of sand

Test	Experimental value
Specific gravity, G_s	2.70
Effective size, D_{10} (mm)	0.16
Effective size, D_{30} (mm)	0.42
Effective size, D_{60} (mm)	1.61
Uniformity coefficient, C_u	10.06
Coefficient of gradation, C_c	0.68
Unified soil classification System, USCS	SW

Table 2 Chemical ingredients for sodium silicate grout

Material	Silicon dioxide (SiO_2) (%)	Sodium dioxide (Na_20) (%)	Moisture (%)	Iron (Fe) (%)	Insolubility (%)
Sodium silicate (No.3)	28.8	9.17	64.2%	0.012	0.072

2.2 Sodium silicate grout, cement grout, and sodium silicate-cement grout

Sodium silicate composed silica sand (SiO_2) and soda ash (Na_2CO_3) are heated at a temperature of 1100-1200°C. The resulting glass can be dissolved using high-pressure steam to form a clear, slightly viscous liquid known as "waterglass". The molecular ratio (R_p = SiO_2/Na_2O) is greater than or equal to 3. The sodium silicate used in this study was manufactured by Pinnacle Industrial Co. Ltd. The chemical contents of the sodium silicate are reported in Table 2. The sodium silicate was mixed with tap water at a ratio of 1:4 by volume.

Cement grout, CS, contains water and cement. Ordinary Portland cement (OPC) was used in this study. The water to cement ratio by weight is set at 0.5. The OPC was manufactured by the Taiwan Cement Corporation. The chemical contents and the basic physical properties of cement are presented in Tables 3 and 4, respectively.

Sodium silicate-cement grout, SCG, is a mixture of the chemical combination of the sodium and cement solutions. The ratio of sodium silicate grout to cement grout is 1:1.

Table 3 Chemical content of OPC (%)

Ingredient	SiO_2	Al_2O_3	Fe_2O_3	CaO	MgO	$S0_3$	Na_2O	K_2O
OPC (type 1)	21.24	4.44	3.44	64.51	2.35	2.10	0.18	0.59

Table 4 OPC physical properties

Ingredient	Specific gravity	Fineness (cm^2/g)	Loss on Ignition (%)	Insolubility (%)	Alkali content (%)	Initial setting time (min.)	Final setting time (min.)
OPC (type 1)	3.16	3490	0.98	0.12	0.57	139	255

3. Sample preparation and tests

3.1 Sample preparation

In this study, a specimen of 7.0 cm in diameter and 15.0 cm in height was prepared using the wet tamping method. For clean sand, the dry clean sand was first divided into five equal parts. Each part was added to an amount of de-aired water and mixed into the wet mixture with an exact water content of 8% (Ishihara 1993). Then, each part was placed in a mold covered by a rubber membrane and compacted to a given height. Finally, to obtain a good contact between the layers, the surface of each tamping layer was roughened to a depth of 5 mm using a knife. The same initial dry densities were maintained during test preparation: $Dr = 30 \pm 2\%$.

Similarly, for grouted sand, the sand specimens were mixed with 3.5 and 5% grout by volume, respectively. The specimen was mixed with either sodium silicate grout or cement grout or sodium silicate-cement grout. To obtain a specimen with a relative density of 30 ± 2%, the dry sand sample was also divided into 5 equal parts, and each part was added to the exact grout volume. The mixture was carefully poured into a split-mold covered paper mold around the side. Each part was compacted to a selected height. Then, the specimen-covered paper mold was moved into a water tank to complete curing. After reaching the curing time, the specimen was placed in the bottom of the cell of the testing equipment. Finally, the paper mold was torn, and the rubber membrane was set using the copper-mold before conducting the test, as indicated in Fig. 2.

After the sample was completely cured, the specimen was consequently saturated by flowing carbon dioxide, CO_2, for at least 60 minutes, and de-aired water was allowed to flow through the specimen from bottom to top to ensure that Skempton's coefficient B was equal to 0.95 or greater at the end of the saturated stage. In this study, a backpressure of 200 kPa has been applied during the test to reach the saturated state. After the saturation process, the specimens were subjected to a confining pressure for consolidation. During consolidation, the difference between the confining pressure and the backpressure was established such that, for each sample, the effective consolidation pressure was fixed at 50, 100, and 200 kPa. The grouted specimens were tested using cyclic triaxial and resonant column tests with various grout contents for curing times of 3, 7, 28 and 91 days.

3.2 Cyclic triaxial test

The cyclic triaxial tests were conducted in accordance with ASTM D5311-2013, which used an

(a) Tearing the paper mold (b) Setting the rubber membrane

Fig. 2 Sample preparation

Fig. 3 Dynamic triaxial test

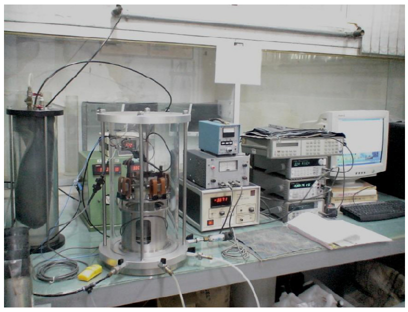

Fig. 4 Resonant column test

automatic triaxial test system, as indicated in Fig. 3. This testing equipment, i.e., the CKC cyclic triaxial device, was fabricated by the Soil Equipment Company (San Francisco, CA, USA). During cyclic axial loading, a sinusoidal loading was applied to the saturated specimens. The variation in the excess pore water pressure, axial stress, and axial strain of the specimen were recorded during cyclic loading. The frequency of cyclic loading was fixed at 1 Hz. The results were characterized in terms of the cyclic stress ratio (CSR), which was defined as the peak shear stress ($\sigma_d/2$) divided by the initial effective consolidation stress, σ'_c. A series of cyclic triaxial tests were conducted on various grout types and grout contents of specimens at an effective confining pressure of 100 kPa to determine the liquefaction resistance.

$$CSR = \frac{\sigma_d}{2\sigma'_c} \tag{1}$$

3.3 Resonant column test

The resonant column apparatus was manufactured by Structural Behavior Engineering Laboratory Inc, 4236 N 39th Avenue Phoenix, AZ 85019 and is also known as the Stokoe torsional shear/ resonant column device, as indicated in Fig. 4. The measurements of the shear modulus and the damping ratio were obtained using the resonant column test based on ASTM D4015-2007. The device is a fixed-free system consisting of a cylindrical specimen that has platens attached to each end. During the resonant column test, a sinusoidal vibration excitation device with a frequency ranging from 2 Hz to 60 Hz is applied to the top of the specimen. The above testing description corresponds to a cyclic torque of constant amplitude and varying frequency being applied to the top of the specimen. Variations in the peak torsional displacements with a change in frequency were recorded, and the frequency response curve was drawn. The resonant frequency corresponding to the peak of the curve was then determined. From these recorded data, the shear small-strain, maximum shear modulus, and shear modulus of soils can be obtained. In addition, the values of damping ratio were determined by recording the free decaying vibrations of the specimen when the electromagnetic drive system was shut-off. Similarly, the amplitude of vibration gradually increased stepwise; a new resonant frequency and decay pattern were obtained in each step, and results of dynamic properties were thus obtained. To investigate the effect of confining pressure on the dynamic properties of specimens, three levels of confining pressure of 50, 100 and 200 kPa were applied to each specimen.

4. Test results and discussions

4.1 Microstructure study

The microstructure of a material has an interdependence on the physical and mechanical properties, such as water retention, compressive and tensile strength, Young's modulus, and Poisson's ratio (Taylor 1998). For the different grouts, the change in microstructure has been attributed to the chemical composition, such as sodium silicate and cement. The microstructure study was only performed on an optical electron microscope (environment optical microscope-EOM) to understand the different microstructures between the clean sand and silicate-cement grouted sand for a 91-day curing time. It can be clearly observed from Fig. 5(a) that the clean sand includes round spherical-shaped particles that surround the void; the grey color of the grain is obtained in this type, and it is highly unlikely for interconnections to occur between particles. Conversely, the silicate-cement grouted sand indicates that the surface of the particle is covered by a white layer surrounding the sand particle; the density of the grouted sand appears to be denser and the voids decrease, as indicated in Fig. 5(b). This phenomenon can be explained in the following manner: calcium hydroxide is produced by mixing cement with water. Then, hydrated sodium silicate and a gel form of sodium silicate is produced by the neutralization.

4.2 Cyclic triaxial test

It is necessary to evaluate the liquefaction resistance of clean sand and grouted sand. The cyclic triaxial test was conducted on specimens mixed with various grout contents of 3.5 and 5% at the age of 3, 7, 28, and 91 days. This test was performed on ninety-three specimens. The data were recorded at a double deformation of 2.5%, 5%, and 10% and reached initial liquefaction. In this study, the initial liquefaction is defined as the number of cycles required where the excess pore water pressure reaches a value just equal to the effective confining pressure or 5% double deformation axial strain, whichever occurs first (Mominul *et al*. 2013).

Fig. 6(a) presents the typical hysteresis loops and relationships between the deviator stress and the axial strain, the axial strain and the number of cyclic loadings, and the pore water pressure and the number of cyclic loadings for clean sand. Specimens treated with sodium silicate grout have the same tendencies and are not shown herein. Although the specimens were tested with different

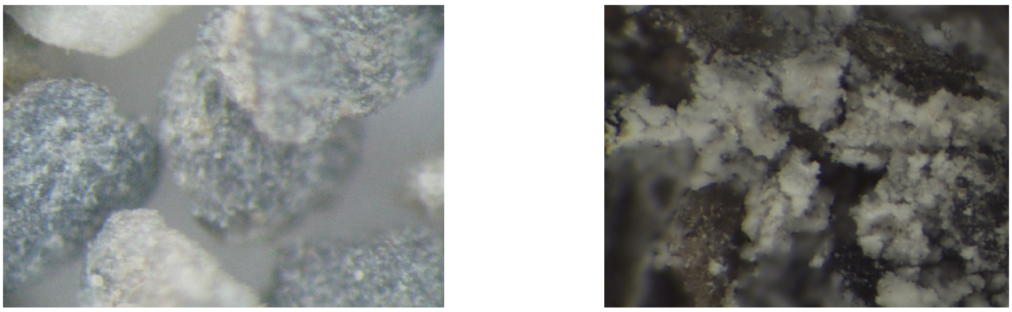

(a) (b)

Fig. 5 Particle surface of material (a) clean sand; and (b) sodium silicate-cement grouted sand, magnified X600

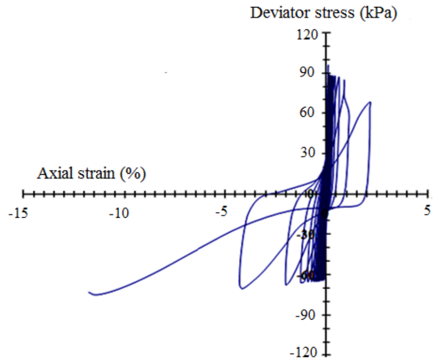

Hysteresis loop

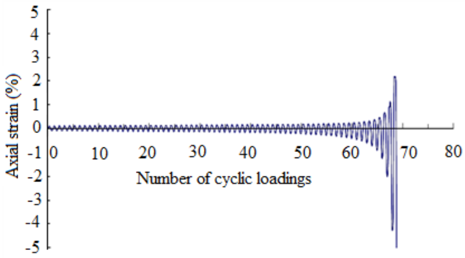

Variation of axial strain with number of cyclic

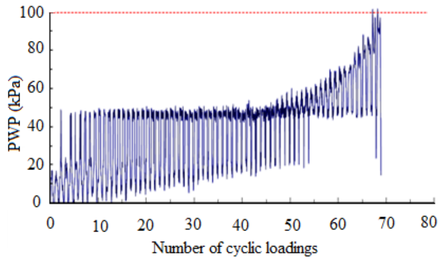

Variation of PWP with number of cyclic loadings

(a) Clean sand sample (CSR = 0.35)

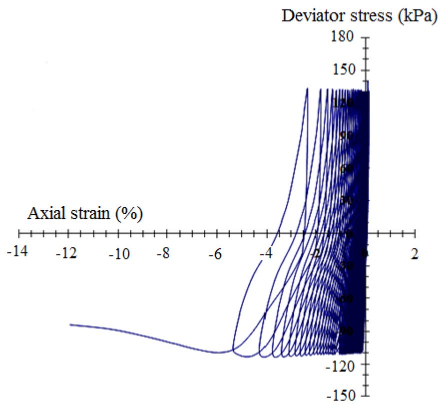

Hysteresis loop

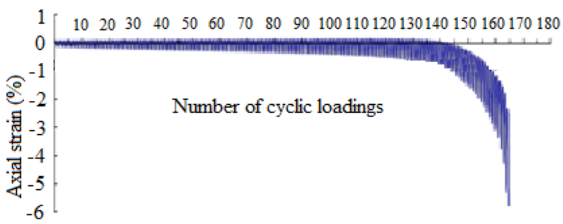

Variation of axial strain with number of cyclic loadings

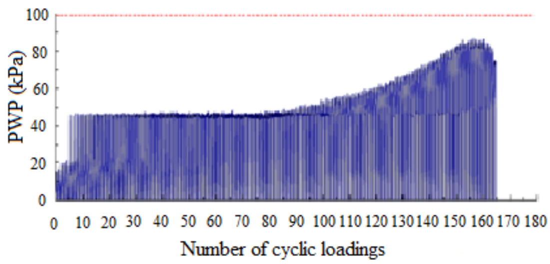

Variation of PWP with number of cyclic loadings

(b) Cement grouted sand (CSR = 0.54)

Fig. 6 Results of cyclic triaxial test

cyclic stress ratios, the clean sand and the sodium silicate grouted sand have the same behavior for relationships between the axial strain-number of cyclic loadings and the pore water pressure PWP-number of cyclic loadings. Both positive and negative deformations are obtained during the testing procedure; the pore water pressure can reach the effective confining pressure. Specifically, once the double deformation reaches the 5% axial strain, the pore water pressure also appears to reach the effective confining pressure simultaneously, and thereafter the failure of specimens occurs rapidly with an increase in further cyclic loadings.

Additionally, a typical result of cyclic triaxial test on a cement grouted sand. Because specimens treated with sodium silicate-cement grouted sand have the same tendencies and are thus not presented. Although a greater CSR is used to test cement grouted sand compared with that of sodium silicate-cement grouted sand, the cement grouted sand has a greater number of cyclic loadings that cause initial liquefaction than does sodium silicate-cement grouted sand. Particularly, the pore water pressure of cement grouted sand cannot reach the confining pressure during the test whereas the pore water pressure of sodium silicate grouted sand can still reach the effective confining pressure during the testing procedure. Compared with Fig. 6(a), the results indicate that the specimens grouted with cement grout or sodium silicate grout significantly increase the liquefaction resistance by increasing the stiffness caused by the hydration of the cement grout as well as the sodium silicate-cement grout.

Fig. 7 presents the result of the relationship between the cyclic stress ratio (CSR) and the number of cyclic loadings (Nos) for the initial liquefaction stage of all specimens. To estimate the liquefaction resistance of specimens subjected to an earthquake of 7.5 magnitude, the liquefaction resistance is defined as the cyclic stress ratio requirement to cause initial liquefaction in 15 cycles

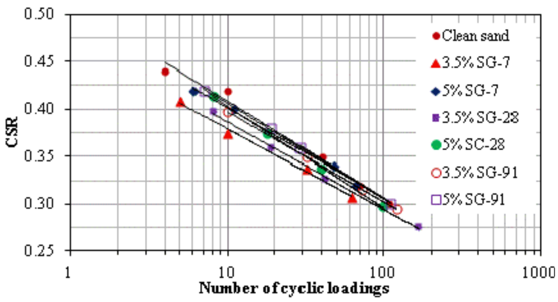

(a) Sodium silicate grouted sand

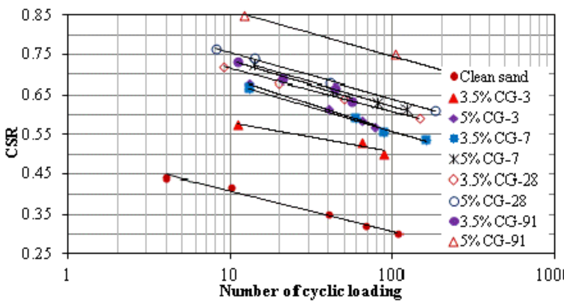

(b) Cement grouted sand

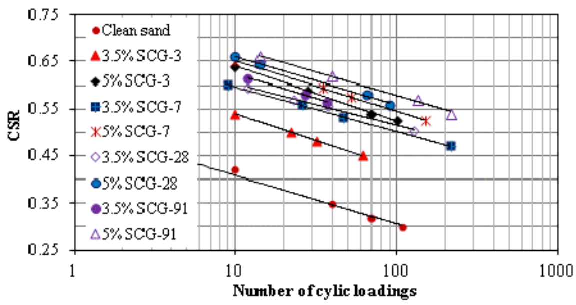

(c) Sodium silicate-cement grouted sand

Fig. 7 Cyclic stress ratio versus number of cyclic loadings of loading (Das and Ramana 2010). It is essential to compare the liquefaction resistance between clean sand and grouted sand, and the ratio of CRR (RCRR) was, therefore, defined as the rate of the cyclic resistance ratio of grouted sand relative to that of clean sand, as given in Eq. (2).

$$RCRR = \frac{CRR\ of\ grouted\ sand}{CRR\ of\ clean\ sand} \tag{2}$$

Fig. 8 describes the ratio of cyclic resistance ratio for various grouted sands at different curing times. Fig. 8(a) provides the various ratios of cyclic stress ratios for a grout content of 3.5%. Based on the results of sodium silicate grouted sand, the specimen cannot be tested at a 3-day curing time because of the weak strength of the specimen with a grout content of 3.5%. The ratio of cyclic resistance ratio slowly increases with the curing time and is less than 1, even up to a curing time of 91 days. This result occurred because as the specimen was added to the sodium silicate, the mixture became more viscous and weak, and the internal structure significantly changed the bond of the specimen. It can be concluded that only using sodium silicate without a hardener cannot improve the liquefaction resistance of the mixture.

The specimen-grouted cement grout significantly increases the RCRR within an early curing time; however, after 28 days of curing, the RCRR slowly increases with further increases in the curing period. The cement grouted sand exhibited an RCRR 1.45 to 1.82 times larger than that of clean sand. The reason for this result is that the stiffness of the specimen improves the strength with an increase in the number of curing days. Furthermore, the increased tendency is in agreement with the observations of a few previous researchers (Dupas and Pecker 1979, Haeri *et al*. 2005, Saxena *et al*. 1988b). Conversely, the mixture containing sodium silicate and cement grout still increases with a further increase in curing time after curing for 28 days. Furthermore, the sodium silicate-cement grouted sand increases the RCRR in the range of 1.33 to 1.55 times with a curing time of 3 to 91 days.

Fig. 8(b) presents the RCRR for specimens containing a grout content of 5%. The results revealed that the RCRR of sodium silicate grouted sand still has a tendency to slowly increase with an increase in curing time. The RCRR of cement grouted sand substantially develops with increasing curing age; the RCRR still increases after 28 days of curing. Furthermore, the RCRR of sodium silicate-cement grouted sand increases with a curing time from 3 to 28 days; thereafter, it slowly increases with a further increase in curing days. The results indicate that when increasing the grout content in the mixture to 5%, the effects of sodium silicate grout are inconsiderable on the liquefaction resistance of the sodium silicate-cement grouted sand, and the cement grout plays a more important role in the mixture.

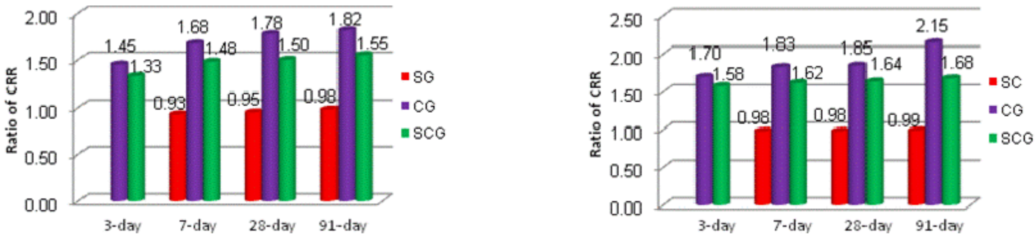

(a) Grout content of 3.5% (b) Grout content of 5%

Fig. 8 Ratio of cyclic resistance ratio versus curing time

4.3 Resonant column test

The resonant column test was performed on twenty-three specimens. The grouted sand was tested after 3, 7, 28, and 91 days of curing. During the test, each specimen was not to be destroyed with the range of investigated strain; therefore, each specimen was tested with three types of effective confining pressure of 50, 100, and 200 kPa.

4.3.1 Shear modulus

The results in the variation of shear modulus with shear strain for different grout contents are presented in Fig. 9. Generally, the results indicate that the shear modulus decreases with an increase in shear strain. The decrease in shear modulus tends to exhibit nonlinear behavior for both clean and grouted sand. The trends obtained in this study are also well-known shear modulus-shear strain relations and are in agreement with a few previous researchers (Ansal *et al*. 2001, Delfosse-Ribay *et al*. 2004, Saxena *et al*. 1988a). The loss of stiffness in the mixtures is most likely attributable to the weakening of the structure between the particle and the grout. This phenomenon can be attributed to the worsening bond between the grains of sand particle and the grout that occurs as the shear strain increases. For a larger shear strain, the shear modulus has the declining tendency to converge into that of clean sand, and the behavior of grouted sand is similar to that of clean sand. Particularly, it should be noted that for a shear strain less than 8×10^{-4} (%), the shear modulus appears to remain at a constant value; thus, the maximum shear modulus can be determined by this range of strain. For all specimens, the elastic zone is obtained, and the cement

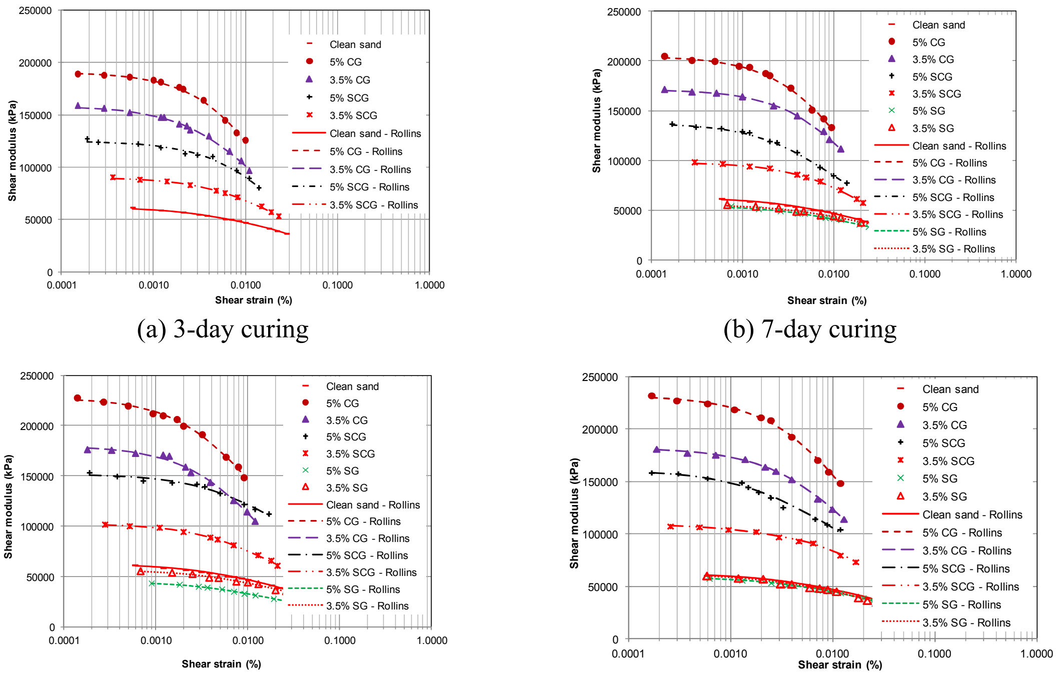

(a) 3-day curing

(b) 7-day curing

(c) 28-day curing

(d) 91-day curing

Fig. 9 Variation of shear modulus with shear strain grouted sand has a smaller strain compared with those of both sodium silicate-cement grouted and clean sand.

Fig. 10 provides the typical effects of effective confining pressure on the shear modulus. It is evident that the shear modulus of sand grouted sodium silicate and clean sand have the same tendency; the tendency of shear modulus for the sand grouted sodium silicate-cement is similar to that of sand grouted cement grout, and it is thus not drawn herein. As displayed in Fig. 10, the effect of confining pressure is more considerable for cement grouted sand and sodium silicate-cement grouted sand than for sodium silicate grouted sand and clean sand. If a greater confining pressure is applied, the shear modulus is greater. For a higher confining pressure, the interconnection between particles is denser, and the stiffness of the material increases significantly. Previously, a few researchers revealed that the shear modulus of clean sand remarkably depends on the confining pressure and void ratio, and an increase in the shear modulus of grouted sand is primarily due to being dependent on void ratio, cement content, and effective confining pressure (Haeri *et al*. 2005, Saxena *et al*. 1988a).

It is essential to estimate the effect of the type and content of different grouts on the shear modulus. For sodium silicate grout, it can be noted that there is no improvement in the shear modulus with an increase in sodium silicate content from 3.5 to 5%. This result indicates that sodium silicate grout without any hardener cannot be used to improve the stiffness of the sand or the shear modulus. For the cement-grouted sand, the results also indicate that the shear modulus remarkably increases with an increase in the cement grout content from 3.5% to 5% when controlling other parameters.

Furthermore, the shear modulus of the sodium silicate-cement grouted sand depicts a similar trend when compared with that of the cement grouted sand. At the same gout content, the shear

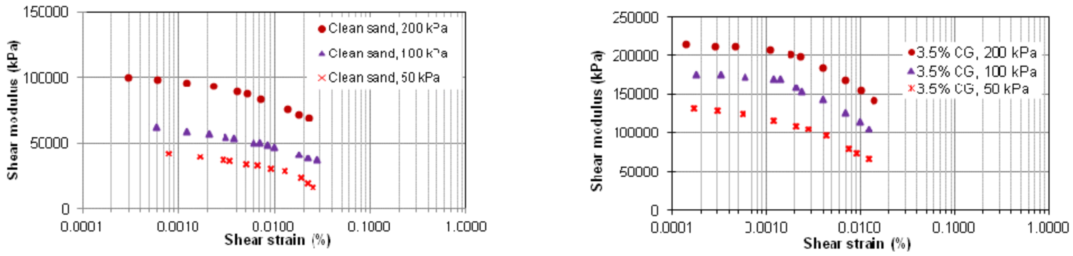

(a) Clean sand (b) Cement grouted sand at 28 days

Fig. 10 Variation of shear modulus with various confining pressures

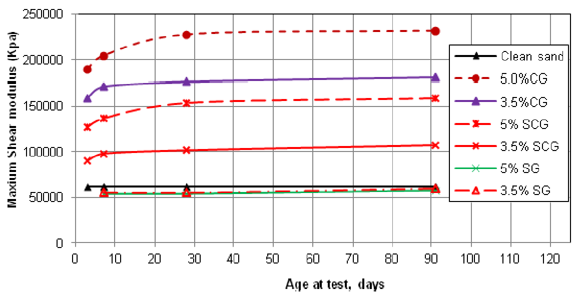

Fig. 11 Variation of maximum shear modulus with curing age

modulus of the sodium silicate-cement grouted sand is less than that of the cement grouted sand. Generally, the results in this study tend to agree with the observations of previous studies (Delfosse-Ribay *et al*. 2004, Haeri *et al*. 2005, Maher *et al*. 1994a, Pantazopoulos and Atmatzidis 2012).

Fig. 11 provides the relationships between the maximum shear modulus, Gmax, and curing time for different grout types. The results indicate that the maximum shear modulus for sodium silicate grouted sand with various grout contents is less than that of clean sand. Conversely, the sand grouted with either cement or sodium silicate-cement grout describes an increased tendency in the maximum shear modulus; for a higher grout content, the maximum shear modulus is greater. An increase in the maximum shear modulus of up to 1.4- to 2.6-fold for 3.5 and 5% sodium silicate-cement grouted sand is obtained compared with that of clean sand. The average improvement factors are 2.5 and 3.7 times for sand grouted with 3.5 and 5% cement grout, respectively.

Additionally, the maximum modulus of cement grouted sand increases with an increase in curing time from 3 to 28 days. This result is due to the hydration of cement; the bond becomes stronger. For a longer curing time of up to 91 days, the maximum shear modulus and shear modulus slowly decrease. For sodium silicate-grouted sand, the maximum shear modulus and shear modulus still tend to increase with a curing time from 3 to 91 days.

The normalized shear modulus has been studied by several researchers not only for soil but also for grouted material (Acar and El-Tahir 1986, Delfosse-Ribay *et al*. 2004, Rollins *et al*. 1998, Stokoe *et al*. 1999, Wang and Kuwano 1999). In this study, for the normalized shear modulus of all of the various grouted sands, a hyperbolic law proposed by the Rollins *et al*. (1998) and Delfosse-Rebay *et al*. (2004), namely Rollins-Delfosse-Rebay law, is used to investigate the result of normalized shear modulus with the shear strain, as shown in Eq. (3)

$$\frac{G}{G_{\max}} = \frac{1}{A + B \times \gamma \times (1 + 10^{(C \times \gamma)})} \tag{3}$$

where $G_{\max}$ is the maximum shear modulus; G is the shear modulus; γ is the shear strain; and A, B and C are constant values.

To investigate the distribution of experimental data, a coefficient of determination, R^2, is proposed. The coefficient of determination is the proportion of variability in a data set that is accounted for by a statistical model. In this definition, the term “variability” is defined as the sum of squares. There are equivalent expressions for R^2 based on the analysis of variance decomposition.

The results used a nonlinear regression method to determine A, B, C and the R-squared coefficient of determination, as presented in Table 5. The results indicate that the normalized shear modulus obtained in this study is in good agreement with the hyperbolic law proposed by Rollins-Delfosse-Rebay. The coefficients of determination are nearly greater than 0.984. The results of the shear modulus using the Rollins-Delfosse-Rebay method are plotted in Fig. 9, and it is evident that the curves for the shear modulus describe the best performance with the obtained data in this study. The result of the normalized shear modulus are also in agreement with the previous study performed by (Delfosse-Ribay *et al*. 2004), who determined the normalized shear modulus for various grouted sands.

Table 5 Rollins-Delfosse-Rebay law constants and R-squared for various grouted sands

Types of grout	Constants and R-squared			
	A	B	C	R^2
Clean sand	0.988	24.432	- 48.280	0.997
Sand + 3.5% silicate grout, 7 days curing	0.983	19.836	- 36.372	0.993
Sand + 3.5% silicate grout, 28 days curing	0.976	20.063	- 32.077	0.991
Sand + 3.5% silicate grout, 91 days curing	0.973	28.895	- 67.392	0.993
Sand + 5.0% silicate grout, 7 days curing	0.991	22.501	- 35.702	0.991
Sand + 5.0% silicate grout, 28 days curing	0.961	22.492	- 23.281	0.996
Sand + 5.0% silicate grout, 91 days curing	0.980	22.418	- 46.072	0.998
Sand + 3.5% cement grout, 3 days curing	1.001	31.311	- 9.122	0.996
Sand + 3.5% cement grout, 7 days curing	0.999	23.027	- 2.666	0.998
Sand + 3.5% cement grout, 28 days curing	0.979	31.364	- 5.734	0.993
Sand + 3.5% cement grout, 91 days curing	0.993	25.880	- 8.134	0.999
Sand + 5% cement grout, 3 days curing	0.989	23.134	12.109	0.997
Sand + 5% cement grout, 7 days curing	0.995	28.627	1.654	0.997
Sand + 5% cement grout, 28 days curing	1.001	33.907	-19.885	0.996
Sand + 5% cement grout, 91 days curing	0.999	26.106	-6.404	0.998
Sand + 3.5% silicate-cement grout, 3 days curing	0.997	17.754	-7.003	0.998
Sand + 3.5% silicate-cement grout, 7 days curing	0.996	18.305	-3.769	0.999
Sand + 3.5% silicate-cement grout, 28 days curing	0.992	20.424	-13.324	0.998
Sand + 3.5% silicate-cement grout, 91 days curing	0.982	28.919	-149.368	0.996
Sand + 5% silicate-cement grout, 3 days curing	1.016	18.367	3.928	0.987
Sand + 5% silicate-cement grout, 7 days curing	0.988	39.282	- 24.470	0.998
Sand + 5% silicate-cement grout, 28 days curing	1.011	16.597	- 29.123	0.984
Sand + 5% silicate-cement grout, 91 days curing	0.986	43.107	- 71.042	0.985

4.3.2 Damping ratio

The resonant column test was used to determine the damping ratio. The resonant frequency was obtained, the excitation was suddenly turned off, and the specimen was subjected to free oscillation. The damping ratio was determined based on the free-vibration curve using the logarithmic decrement method (Das and Ramana 2010), as indicated in Eq. (4)

$$D(\%) = \frac{1}{2\pi n}\ln\left(\frac{A_0}{A_n}\right) \tag{4}$$

where A_0 is the vibration amplitude of the first cycle after the excitation has been turned off; A_n is the vibration amplitude of the n^{th} cycle; and n is the number of cycles in free vibration.

The results of the damping ratio are expressed in Figs. 12(a)-(d). The results indicate that the damping ratio increases nonlinearly with an increase in the shear strain. The primary reason for this result is that an increase in the damping ratios is caused by the energy absorption caused by

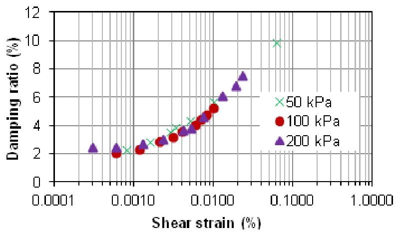

(a) Clean sand

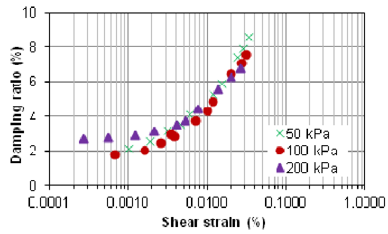

(b) Sodium silicate grouted sand

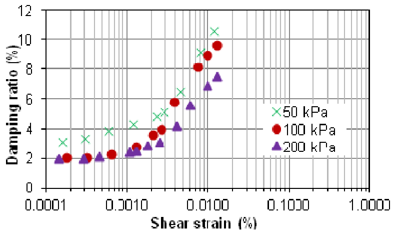

(c) Cement grouted sand

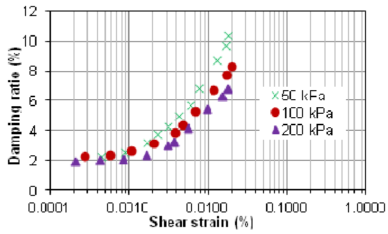

(d) Sodium silicate-cement grouted sand

Fig. 12 Variation of damping ratio with confining pressure, at the curing age of 28-day

particle rearrangement. Figs. 12(a) and (b) indicate that the effective confining pressure has no significant effects on damping for clean sand or sodium silicate grouted sand. The results also agrees with the results of (Delfosse-Ribay *et al*. 2004) and (Maher *et al*. 1994b). However, Figs. 12(c) and (d) indicate that the damping ratio of both sodium silicate-cement grouted sand and cement grouted sand decrease with an increase in the effective confining pressure. The reason for this result is because for a higher effective confining pressure, the interconnection of the grain is higher, there are significantly more pathways and less energy is expected to be dissipated during the propagation (Saxena *et al*. 1988a). Additionally, the damping ratio for all of the specimens insignificantly increases for a range of strain smaller than 10^{-3}(%); for higher strains, the damping ratio remarkably increases to reach an average improvement value of 3 to 4 times compared with that of small shear strain.

The clean sand presents a narrow distribution of the damping ratio with an increase in shear strain; the damping ratios obtained using confining pressures of 100 kPa and 200 kPa are inconsiderably different for a shear strain higher than 2×10^{-3} (%). The sodium silicate grouted sand describes a large scatter in the damping ratio with a shear strain smaller than 3×10^{-3} (%). For a higher shear strain, the damping ratio is arranged in a narrow band. Both the sodium silicate-cement grouted sand and the cement grouted sand indicate the same trend in the increase of the damping ratio with a decrease in confining pressure, and the values of damping ratios are also distinguished with the confining pressure.

A specific shear strain of 8×10^{-4} (%) is selected to investigate the damping ratio with an increase in the confining pressure, as indicated in Fig. 13. Both the clean sand and the sodium silicate grouted sand describe the decreased trend in damping ratio with a confining pressure of 50 to 100 kPa; thereafter, the damping ratio increases with a further increase in the confining pressure. Conversely, a decreasing trend in the damping ratio is obtained with the cement grouted sand as well as the sodium silicate grouted sand. It can be noted from Fig. 13 that the damping ratio reaches a value of 2.35% for all specimens with a confining pressure of 150 kPa.

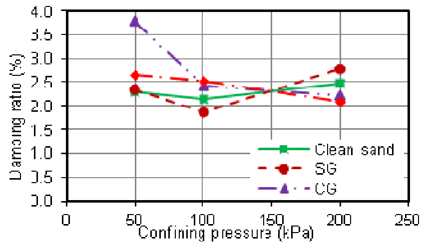

Fig. 13 Variation of damping ratio with confining pressure for shear strain of 8×10^{-4} (%)

5. Conclusions

The liquefaction resistance and the dynamic properties of sodium silicate, cement, and sodium silicate-cement grouted sand were investigated using the cyclic triaxial and resonant column tests. The effects of shear strain, effective confining pressure, type of grout, grout content and curing period were evaluated in this study. Based on the obtained results, the following conclusions were drawn:

- Using only sodium silicate grout may not improve the cyclic stress ratio, shear modulus or damping ratio of sandy soil. Conversely, using cement or silicate-cement grout significantly increases the cyclic stress ratio and the shear modulus of sandy soil. The cement grouted sand exhibited an RCRR 1.45 to 2.15 times larger than that of clean sand, and an increase in the RCRR of 1.33- to 1.68-fold for sodium silicate-cement grouted sand is obtained compared with that of clean sand.
- The maximum shear modulus of cement grouted sand increases with a curing time from 3 to 28 days whereas the maximum modulus of sodium silicate-cement grout sand increases with an increase in curing time of up to 91 days. An increase in the maximum shear modulus of up to 1.4-2.6 times for 3.5 and 5% sodium silicate-cement grouted sand is obtained compared to that of clean sand. An improvement factor of 2.5 and 3.7 is obtained for sand grouted with 3.5 and 5% cement grout, respectively.
- The results of the normalized shear modulus are well distributed based on the hyperbolic law of Rollins-Delfosse-Rebay. The coefficients of determination, R^2, are nearly greater than 0.984. The data are helpful for calculating the related geotechnical problems within a range of small shear strain.
- The confining pressure has no remarkable effect on the damping ratio for clean sand and sodium silicate grouted sand whereas the damping ratios of both cement grouted sand and sodium silicate-cement grout sand decrease with an increase in the confining pressure.

References

ASTM D422-2007 (2007), Standard Test Method for Particle-Size Analysis of Soils, West Conshohocken, PA, USA.
ASTM D2487-2000 (2010), Standard Practice for Classification of Soils for Engineering Purposes (Unified Soil Classification System), West Conshohocken, PA, USA.
ASTM D4015-2007 (2010), Standard Test Methods for Modulus and Damping of Soils by Resonant-

Column Method, West Conshohocken, PA, USA.
ASTM D854-2010 (2010), Standard Test Methods for Specific Gravity of Soil Solids by Water Pycnometer, West Conshohocken, PA, USA.
ASTM D5311-2013 (2013), Standard Test Method for Load Controlled Cyclic Triaxial Strength of Soil, West Conshohocken, PA, USA.
Acar, Y.B. and El-Tahir, A. (1986), "Low strain dynamic properties of artificially cemented sand", *J. Geotech. Eng, ASCE*, **112**(11), 1001-1015.
Ansal, A., İyisan, R. and Yıldırım, H. (2001), "The cyclic behaviour of soils and effects of geotechnical factors in microzonation", *Soil Dyn. Earthq. Eng.*, **21**(5), 445-452.
DOI: http://dx.doi.org/10.1016/S0267-7261(01)00026-4
Chang, T. and Woods, R. (1987), "Effect of confining pressure on shear modulus of cemented sand", *Soil Struct. Interact.*, 193-208.
Chen, J.W. and Lin, C.Y. (2003), "Cemented behavior of hydraulic fill material", *Proceedings of the 13th International Offshore and Polar Engineering Conference*, Honolulu, HI, USA, May, pp. 432-439.
Das, B.M. and Ramana, G.V. (2010), *Principles of Soil Dynamics*, (2nd ed.), Cengage Learning.
Delfosse-Ribay, E., Djeran-Maigre, I., Cabrillac, R. and Gouvenot, D. (2004), "Shear modulus and damping ratio of grouted sand", *Soil Dyn. Earthq. Eng.*, **24**(6), 461-471.
DOI: http://dx.doi.org/10.1016/j.soildyn.2004.02.004
Dupas, J.M. and Pecker, A. (1979), "Static and dynamic properties of sand-cement", *J. Geotech. Eng. Div., ASCE*, **105**(5), 419-436.
Gallagher, P.M. and Mitchell, J.K. (2002), "Influence of colloidal silica grout on liquefaction potential and cyclic undrained behavior of loose sand", *Soil Dyn. Earthq. Eng.*, **22**(9-12), 1017-1026.
DOI: http://dx.doi.org/10.1016/S0267-7261(02)00126-4
Gonzalez, H. and Vipulanandan, C. (2007), "Behavior of a sodium silicate grouted sand", *Proceedings of Geo-Denver 2007*, Denver, CO, USA, February, pp. 1-10.
Haeri, S.M., Hosseini, S.M., Toll, D.G. and Yasrebi, S.S. (2005), "The behaviour of an artificially cemented sandy gravel", *Geotech. Geol. Eng.*, **23**(5), 537-560.
Hsiao, D.H., Phan, T.A.V. and Huang, C.C. (2014), "Liquefaction resistance of grouted sand", *Proceedings of International Conference on Energy, Environment and Materials Engineering* (*EEME 2014*), Shenzhen, China, February.
Ishihara, K. (1993), "Liquefaction and flow failure during earthquakes", *Geotechnique*, **43**, 351-451.
Kazemian, S., Prasad, A., Huat, B.B.K., Ghiasi, V. and Ghareh, S. (2012), "Effects of cement–sodium silicate system grout on tropical organic soils", *Arab. J. Sci. Eng.*, **37**(8), 2137-2148.
DOI: 10.1007/s13369-012-0315-1
Liao, H.J., Huang, C.C. and Chao, B.S. (2004), "Liquefaction resistance of a colloid silica grouted sand", *Proceedings of the 3rd International Conference on Grouting and Ground Treatment*, New Orleans, LA, USA, February, pp. 1305-1313.
Maher, M.H., Ro, K.S. and Welsh, J.P. (1994a), "Cyclic undrained behavior and liquefaction potential of sand treated with chemical grouts and Microfine Cement (MC-500)", *Geotech. Test. J.*, **17**(2), 159-170.
Maher, M.H., Ro, K.S. and Welsh, J.P. (1994b), "High strain dynamic modulus and damping of chemically grouted sand", *Soil Dyn. Earthq. Eng.*, **13**(2), 131-138.
DOI: http://dx.doi.org/10.1016/0267-7261(94)90005-1
Mollamahmutoglu, M. and Yilmaz, Y. (2011), "Engineering properties of medium-to-fine sands injected with microfine cement grout", *Mar. Georesour. Geotechnol.*, **29**(2), 95-109.
Mollamahmutoglu, M., Yilmaz, Y. and Kutlu, I. (2007), "Grouting performance of microfine cement and sodium silica fume mix into sands", *J. ASTM International*, **4**(4), 1-7.
Mominul, H.M., Alam, M.J., Ansary, M.A. and Karim, M.E. (2013), "Dynamic properties and liquefaction potential of a sandy soil containing silt", *Proceeding of the 18th International Conference on Soil Mechanics and Geotechnical Engineering*, Paris, France, September, pp. 1539-1542.
Pantazopoulos, I.A. and Atmatzidis, D.K. (2012), "Dynamic properties of microfine cement grouted sands", *Soil Dyn. Earthq. Eng.*, **42**, 17-31.

DOI: http://dx.doi.org/10.1016/j.soildyn.2012.05.017

Persoff, P., Apps, J., Moridis, G. and Whang, J. (1999), "Effect of dilution and contaminants on sand grouted with colloidal silica", *J. Geotech. Geoenviron. Eng.*, **125**(6), 461-469. DOI: 10.1061/(ASCE)1090-0241(1999)125:6(461)

Rollins, K., Evans, M., Diehl, N. and III, W. (1998), "Shear modulus and damping relationships for gravels", *J. Geotech. Geoenviron. Eng., ASCE*, **124**(5), 396-405.

Saxena, S.K., Avramidis, A.S. and Reddy, K.R. (1988a), "Dynamic moduli and damping ratio for cemented sands at low strain", *Can. Geotech. J.*, **25**(2), 353-368.

Saxena, S.K., Reddy, K.R. and Avramidis, A.S. (1988b), "Dynamic behavior of artificially cemented sands", *Proceedings of 9th World Conference on Earthquake Engineering*, Tokyo-Kyoto, Japan, August, pp. 41-46.

Sladen, J.A., D'Hollander, R.D. an Krahn, J. (1985), "The liquefaction of sands, a collapse surface approach", *Canadian Geotechnical Journal*, **22**, 564-578. DOI: 10.1139/t85-076

Stokoe, K.H., Darendeli, M.B., Andrus, R.D. and Brown, L.T. (1999), "Dynamic soil properties: Laboratory, field and correlation studies", *Proceedings of the 2nd International Conference on Earthquake Geotechnical Engineering*, Lisbon, Portugal, June, pp. 811-845.

Taylor, H.F.W. (1998), *Cement Chemistry*, (2nd ed.), Thomas Telford, London, UK.

Tsai, P.H. and Ni, S.H. (2012), "Effects of types of additives on dynamic properties of cement stabilized soils", *Int. J. Appl. Sci. Eng.*, **10**(2), 131-144.

Vipulanandan, C. and Ata, A. (2000), "Cyclic and damping properties of silicate-grouted sand", *J. Geotech. Geoenviron. Eng.*, **126**(7), 650-656. DOI: 10.1061/(ASCE)1090-0241(2000)126:7(650)

Wang, G.X. and Kuwano, J. (1999), "Modeling of strain dependency of shear modulus and damping of clayey sand", *Soil Dyn. Earthq. Eng.*, **18**(6), 463-471. DOI: http://dx.doi.org/10.1016/S0267-7261(99)00010-X

Yonekura, R. and Miwa, M. (1993), "Fundamental properties of sodium silicate based grout", *Proceedings of the 11th Southeast Asia Geotechnical Conference*, Singapore, May, pp. 439-444.

CC